International Scientific Journal of Engineering and Management (ISJEM) ISSN: 2583-6129
Volume: 04 Issue: 08 | Aug – 2025 DOI: 10.55041/ISJEM04981
An International Scholarly || Multidisciplinary || Open Access || Indexing in all major Database & Metadata

# An Experimental Investigation of Ultra-High-Performance Concrete Rectangular Columns

[1]Bajirao V Mane, [2]BM Praveen, [3]Uday Kumar G, [4] Amit P. Patil
[1]Post Doctorate Fellow, Department of Civil Engineering, Srinivas University, Institute of Engineering & Technology, Srinivas Nagara, Mukka, Mangaluru, Karnataka, 574146, India
[2,3]Srinivas University, Institute of Engineering & Technology, Srinivas Nagara, Mukka, Mangaluru, Karnataka, 574146, India
[4]Department of Civil Engineering, Rajarambapu Institute of Technology Rajaramnagar, Islampur, Tal. Walwa, Dist. Sangli, Maharashtra, India - 415414. India.

---

**Abstract:**
This study investigates the structural performance of Ultra-High-Performance Reinforced Concrete (UHPRC) rectangular columns under axial, uniaxial, and biaxial loading, with a focus on enhancing strength, ductility, and durability for modern construction. Eighteen columns were fabricated using three concrete grades (M60, M70, M80) and three reinforcement ratios (1.34%, 2.09%, 3.01%), and tested in a 2000 kN capacity loading frame. The effects of material strength, reinforcement content, and load type on load-carrying capacity and failure behavior were systematically assessed. Finite Element (FE) models, comprising 2D plane stress and 3D simulations, were developed and calibrated against experimental results, enabling accurate prediction of peak load, crack propagation, and post-cracking response. Experimental outcomes revealed that higher-grade UHPRC and greater reinforcement ratios substantially improved peak load capacity, post-peak ductility, and energy absorption across all loading conditions. Failure modes displayed gradual post-cracking behavior, highlighting enhanced structural resilience. An analytical load–moment interaction model was formulated and validated with close agreement to experimental and FE findings. The results confirm UHPRC's potential for high-performance structural applications, providing valuable insights for designing strong, ductile, and durable rectangular columns in advanced engineering practice.

**Keywords:** Ultra-High-Performance Reinforced Concrete, rectangular columns, finite element modeling, axial loading, uniaxial bending, biaxial bending.

## 1.INTRODUCTION:

In recent years, Ultra-High-Performance Concrete (UHPC) has gained recognition as a next-generation construction material, offering superior mechanical properties, exceptional durability, and improved structural efficiency compared to conventional and high-strength concrete. With its ultra-dense microstructure, low permeability, and enhanced tensile and compressive strengths, UHPC is particularly suited for applications requiring slender, high-capacity, and long-lasting load-bearing members. The adoption of UHPC has been driven by advancements in material science, such as optimized particle packing, the use of supplementary cementitious materials, and the incorporation of high-range water-reducing admixtures, which collectively enable higher strength and durability without compromising workability. The global demand for space-efficient, resilient, and sustainable infrastructure—especially in high-rise buildings, long-span bridges, and structures in seismic zones—has further underscored the importance of UHPC in modern engineering practice.

While extensive research has been carried out in three primary domains—namely, microstructural composition and material science, mechanical behaviour under various loading conditions, and structural performance in real-world applications—the study of UHPC in reinforced structural members, especially columns, remains a critical area of interest. Columns, being the primary vertical load-bearing elements, are subjected to complex combinations of axial loads and bending moments, particularly in tall structures where slenderness effects and second-order behaviour become significant. The enhanced strength, ductility, and energy absorption capacity of UHPC make it an attractive alternative to conventional concrete for improving the performance of such members while enabling reduced cross-sectional dimensions and greater architectural flexibility.

The present experimental study focuses on the structural behaviour of rectangular slender columns made with Ultra-High-Performance Reinforced Concrete (UHPRC). The columns were designed with a cross-section of 150 mm × 100 mm and an overall height of 1300 mm, reinforced with Fe-415 grade steel. Three UHPC grades—M60, M70, and M80—were employed, with reinforcement ratios of 1.34%, 2.09%, and 3.01%, achieved using 4 longitudinal bars of 8 mm, 10 mm, and 12 mm diameter respectively. A total of 81 columns were fabricated and tested under three loading conditions: pure axial compression, uniaxial bending, and biaxial bending. The selection of different reinforcement ratios and concrete grades allowed a systematic investigation of their influence on load-carrying capacity, failure modes, and ductility characteristics.

The testing program was complemented by advanced finite element (FE) simulations, including both 2D plane stress models and detailed 3D models, calibrated against experimental results. This numerical approach enabled an in-depth

 

understanding of stress distribution, crack initiation, crack propagation, and post-cracking behaviour under various loading conditions. The study also developed an analytical load–moment interaction model for rectangular UHPRC columns, validated against both experimental and FE data. The accuracy of these models provides a practical framework for predicting the performance of UHPC columns in structural design applications.

The experimental findings revealed that higher-grade UHPC and increased reinforcement ratios significantly improved the peak load capacity, post-peak ductility, and energy absorption capacity under all loading conditions. Columns made with M80 UHPC exhibited superior stiffness retention and more gradual post-cracking behaviour, indicating enhanced structural resilience and reduced brittleness compared to lower-grade mixes. Under eccentric loading—both uniaxial and biaxial—the UHPC columns displayed stable load–displacement responses and delayed spalling, highlighting the benefits of UHPC's dense microstructure and higher tensile capacity in controlling crack widening and propagation.

From a practical perspective, the implications of this study are substantial. The improved strength-to-size ratio of UHPC columns allows for the reduction of cross-sectional dimensions without sacrificing load capacity, which is particularly beneficial in high-rise construction where floor space optimization is critical. Moreover, the enhanced ductility and energy dissipation characteristics make UHPC columns more suitable for seismic-resistant design, where the ability to undergo large deformations without sudden failure is essential. The study also confirms that UHPC's low permeability and high durability contribute to longer service life and reduced maintenance requirements, further enhancing its economic and environmental advantages in infrastructure applications.

### 1.1 Slender column:

Slender Columns in Reinforced Ultra-High-Performance Concrete (UHPC) Structures

Compression members are fundamental components in any structural system, primarily designed to carry and transfer axial compressive forces. In reinforced concrete structures, these members are typically represented as columns, which are crucial for the overall load distribution and structural stability. As per IS 456:2000, a column is defined as a compression member with a length exceeding three times its least lateral dimension. These elements play a pivotal role in supporting vertical loads and maintaining structural integrity.

In recent years, the advancement of Ultra-High-Performance Concrete (UHPC) has led to a shift in how compression members—especially slender columns—are designed and evaluated. UHPC's superior mechanical properties, including exceptionally high compressive strength, enhanced tensile behaviour, and superior durability, offer significant advantages when applied to slender reinforced concrete columns.

### 1.2 Significance of the Research:

Over the past decade, Ultra-High-Performance Concrete (UHPC) has emerged as a transformative material in structural engineering, offering exceptional mechanical properties and durability. Advancements in UHPC technology have led to compressive strengths exceeding 150 MPa, enhanced elastic moduli, and significant reductions in structural member sizes, contributing to both material efficiency and architectural flexibility.

### 1.3Advanced Study of Eccentrically Loaded UHPC Columns:

Limited research has been conducted on eccentrically loaded confined concrete columns using Ultra-High-Performance Concrete (UHPC), particularly in examining the influence of strain gradients on the performance of these columns. While earlier studies often assumed a uniform compressive strain distribution across the column cross-section, real-world applications typically involve eccentric loading, which induces significant strain gradients.

Emerging research suggests that the interaction between high-yield strength steel and UHPC is complex, especially under eccentric loading. The use of high-strength steel reinforcement in eccentrically loaded UHPC columns has not always yielded satisfactory ductility or post-peak behaviour. In contrast, exploring alternative materials or fiber-reinforced UHPC solutions may improve energy dissipation and ductile performance, particularly in tension-dominated failure modes.

## 2.0. DESIGN DETAILS OF THE COLUMN UNDER COMPRESSION:

Eighty- One Square reinforced concrete columns measuring 100 mm by 100 mm in section and 1300 mm in height were cast for all grades. The columns were reinforced with four longitudinal steel bars, each with a diameter of 12 mm (1.5%) and a yield strength of 500 MPa. The transverse steel that was provided had 1350 hooks at both ends, a 6 mm diameter at 150 mm c/c, and a yield strength of 500 MPa, as shown in Fig. 4.3.

Because there is almost always some bending, axially loaded columns are uncommon in practice. A load applied with eccentricity is the same as an axial load and total bending moment.

Columns subjected to uni-axial compression are uncommon as long column fails due to bending. A rectangular cross-section with two main bars on both faces of the eccentrically loaded column under compression is used in the present work. Depending on whether the tension steel reaches the yield strength, tension failure or compression failure may take place. However, as the type of collapse is inversely proportional to the axial load, a compression failure might not be prevented by restricting the reinforcement area. To achieve equilibrium conditions, the resultant compressive force Cc + Cs in the section must be equal to act in opposition and act at a point of application of external load Po. When the static equilibrium condition is applied, it follows that the two design strength components are simple to calculate.

$P_u=C_c+C_s$ …….. 5.1

$M_u=Mc+M_s$ …….. 5.2

Where Mc and Ms stand for the centroidal resultant moments caused by Cc and Cs respectively. The following generalized equations for the resultant force in concrete (Cc) and its moment (Mc) concerning the centroidal axis for bending.

$C_c=af_{ck}\,bD$ …….. 5.3

$M_c=C_c\,\{D/2-\bar{x}\}$ …….. 5.4

Where, a = stress block area factor

$\bar{x}$ = distance between the compressed edge and line of action of the centroid of the stress block area.

$a=0.362\,x_u/D$ for $x_u \le D$ …….. 5.5

$a=0.447(1-4g/21)$ for $x_u>D$ …… 5.6

$\bar{x}=0.416x_u$ for $x_u \le D$ …… 5.7

$\bar{x}=\{(0.5-8g/49)*D\}/((1-4g/21)\,)\,0.416x_u$ for $x_u>D$ …… 5.8

where,

$g=16/(7\,x_u/D-3)2$ …….. 5.9

Like the previous example, the following equations for the resultant force in the reinforcement (Cs) and its moment (Ms) about the C.G. of bending.

$C_c=\sum_{(i=1)}^{n}\,[\![(fci-f_{ci})\,A_{ci}]\!]$ …….. 5.10

$M_c=\sum_{(i=1)}^{n}\,[\![(fci-f_{ci})\,A_{ci}\,V_i]\!]$ …….. 5.11

where,

$A_{ci}$= cross-sectional area of reinforcement in the ith row

$y_i$= ith row distance of reinforcement from the centroidal axis, deliberate constructive in the way towards the highly compressed edge

$f$ci = Tensile stress in the reinforcement in the ith row of steel

Ɛci = Strain in the ith row

$f$ci =Compressive stress in the concrete in the ith row.

Equilibrium failure occurs when the ultimate strain reaches the yield point and at some time, the outermost compressive strain reaches 0.003. If Pu < Pb a tension failure occurs and if Pu > Pb, Compression failures occur in the column. A column moment interaction curve is created in the Excel program by referring to the strain profile.

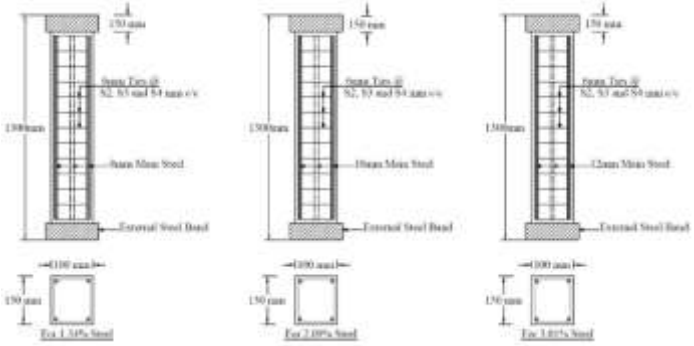

Fig. 1 Rectangular Slender Reinforced UHPC Column Details

## 3.0 SPECIMEN IDENTIFICATION :

The Specimen Identification for different grades of concrete, different loading, and different eccentricities are shown in Table 4.8 and the nomenclature used for column specimens is shown in Table 1.

**Table 1** Details of Rectangular Column Specimens

| Sr. No. | Concrete Grade | Longitudinal Reinforcement | % of Reinforcement | Loading Condition [Column Designation (No.'s)] | | |
|---|---|---|---|---|---|---|
| | | | | **Axial** | **Uni-Axial** | **Bi-Axial** |
| 01 | **M60** | 4# 8mm | 2.01 | R60IA1 (3) | R60IU1 (3) | R60IB1 (3) |
| | | 4# 10mm | 3.14 | R60IIA1 (3) | R60IIU1 (3) | R60IIB1 (3) |
| | | 4# 12mm | 4.52 | R60IIIA1 (3) | R60IIIU1 (3) | R60IIIB1 (3) |
| 02 | **M70** | 4# 8mm | 2.01 | R70IA1 (3) | R70IU1 (3) | R70IB1 (3) |

| | | | | | | |
|---|---|---|---|---|---|---|
| | | 4# 10mm | 3.14 | R70IIA1 (3) | R70IIU1 (3) | R70IIB1 (3) |
| | | 4# 12mm | 4.52 | R70IIIA1 (3) | R70IIIU1 (3) | R70IIIB1 (3) |
| 03 | **M80** | 4# 8mm | 2.01 | R80IA1 (3) | R80IU1 (3) | R80IB1 (3) |
| | | 4# 10mm | 3.14 | R80IIA1 (3) | R80IIU1 (3) | R80IIB1 (3) |
| | | 4# 12mm | 4.52 | R80IIIA1 (3) | R80IIIU1 (3) | R80IIIB1 (3) |

**Nomenclature used for column specimens**

| | |
|---|---|
| R: | Rectangular Column |
| A: | Axially loaded long Column |
| U: | Uniaxial loaded long Column with 20% Eccentricity |
| B: | Biaxial loaded long Column with 20% Eccentricity |
| I: | 2.01% of steel for Square and 1.34% of steel for rectangular columns |
| II: | 3.14% of steel for Square and 2.09% of steel for rectangular columns |
| III: | 4.52% of steel for Square and 3.01% of steel for rectangular columns |
| 60,70,80: | Ultra High-Performance Concrete of grade M60, M70 & M80 |

## 4.0 CASTING OF SPECIMENS:

The same production methods and equipment are used to create UHPCs as conventional strength concrete, as was previously mentioned; the mixing procedure is usually lengthier. To get the intended level of strength, uniformity, and ease of use, all the equipment utilized for measuring and combining the concrete components is accurate and calibrated.

The laboratory utilized a ribbon-type mixer with a capacity of 125 kg for mixing concrete in this experiment. Before casting the specimens, preliminary mixtures were prepared utilizing the previously mentioned elements to get the desired strength of concrete, which ranged from 60 to 80 MPa. The mixtures were subsequently poured into column moulds created of plywood, as seen in Figure 4.4. The material needs of each column were measured and the mixer was filled with roughly 75% water before adding the components. Silica fume, when used as a mineral additive in concrete, was incorporated into the dry aggregates before the addition of water to the mixer. After incorporating the remaining 25% of water, the mixture was gently stirred for a minimum of 10 minutes to achieve a uniform mixture. Before casting the specimen, the workability was evaluated using the slump cone test. The slump values ranged from 100 to 150 mm.

## 5.0 TEST SET-UP AND TESTING PROCEDURE:

The top and bottom ends of the specimens were slightly ground by a grinding machine to remove surface unevenness as shown in Figure 2, but at the same time, it was ensured that excessive grinding was not carried out. In addition, the sheet was kept at the top and bottom ends of the specimens to ensure parallelism of specimen end surfaces and uniform distribution of the load on the specimens. Each specimen end was properly ground after curing to achieve verticality of the specimen in the machine before testing. All of the cylinders' ends were grounded on both sides to make sure they were parallel to the sides.

### 5.1. Column Test Set-up:

The columns were tested in the loading frame of 2000kN capacity with LVDTs attached to extract the longitudinal compression, buckling of columns, and the slip of both ends. To test the column under compression, the top and bottom assembly is made to prevent buckling which is shown in Fig.2. To apply a biaxial load, steel plate provision is made as shown in Fig.3.

International Scientific Journal of Engineering and Management (ISJEM) ISSN: 2583-6129
Volume: 04 Issue: 08 | Aug – 2025 DOI: 10.55041/ISJEM04981
An International Scholarly || Multidisciplinary || Open Access || Indexing in all major Database & Metadata

Mild steel plates measuring 10 mm thick are used to create the top and bottom assembly, which is designed to prevent buckling and is depicted in Fig. 2 to Fig. 10.

**Fig. 2 Top and bottom assembly for column testing**

**Fig. 3 Provision to apply uniaxial and biaxial load.**

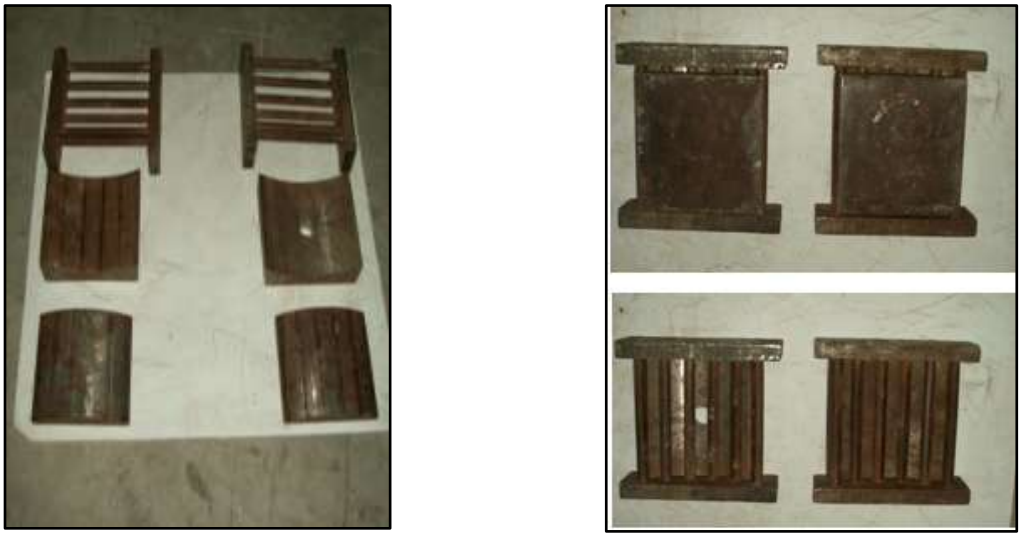

**Fig. 4** Column Boundary Conditions Assembly using Teflon Sheet Plates

### 5.2. Test Set-Up for Columns Subjected to Different Loading:

The specimen's displacement was measured using two linear variable displacement transducers (LVDTs) and dial gauges. One was installed on the opposing faces using steel clamps so that displacement could be continuously measured while the biaxial load was applied. Attached to the bottom was the subsequent LVDT (0-10mm) for tracking the post-peak

displacements. The data acquisition system attached to the loading frame automatically recorded the displacements and loads. In Fig. 4.16, the testing assembly is displayed. The loads were applied using a hydraulic jack with a 2000kN loading frame. Plumb ensured that the column remained vertical Initial crack load, first peak, maximum load, second peak, and corresponding displacements were tracked throughout the testing process. The LVDTs' displacement readings were taken up until the point at which they were freed from the concrete. The data acquisition system is used to extract the data. The load versus deflection and moment interaction curves are plotted using the data that was obtained. The detailed experimental data and the data from the literature can be compared. The findings are confirmed, and conclusions that may provide more understanding of how long columns behave under axial, uniaxial, and biaxial loadings may be drawn.

Using a loading frame with a 2000 kN capacity, the method previously described is used to test various column specimens under axial, uniaxial, and biaxial load. To eliminate surface irregularities and make space for an LVDT arrangement, the specimens' middle surface was slightly ground by a grinding machine. The various arrangements used during the testing of columns under compression are described in Figs. 4.15 to 4.20.

The idea behind this experimental program was to analyse the behaviour of a long, thin column and see what codes were available for predicting the ultimate load and moment. The variables chosen to accomplish this are the concrete's strength (M60 to M80) and various eccentricities of loading (20% of cross-section). Nine columns for each grade totalled twenty-one. The purpose of the research is to examine how eccentricity affects the durability and behaviour of long columns when subjected to axial, uniaxial, and biaxial loads.

Fig. 5 Top Plate Provision for Loading

Fig. 6 Vertical alignment of a column by plumb bob.

International Scientific Journal of Engineering and Management (ISJEM) ISSN: 2583-6129
Volume: 04 Issue: 08 | Aug – 2025 DOI: 10.55041/ISJEM04981
An International Scholarly || Multidisciplinary || Open Access || Indexing in all major Database & Metadata

Fig. 7 Dial Guage Provision

Fig. 8 LVDT Provision.

Fig. 9 Load Applied from the top

Fig. 10 Testing arrangement for the column under biaxial loading.

## 6. THE BEHAVIOUR OF COLUMNS UNDER UNIAXIAL AND BIAXIAL LOADING:

Columns with a longitudinal steel content of 2.01% and a diameter of 8 mm were tested in this study. In general, the behaviour of confined specimens was relatively ductile, even with eccentric columns of 80MPa. These columns exhibited surface cracking, cover spelling, cover separation, longitudinal steel yielding, lateral tie yielding, longitudinal bar buckle

In nearly every column of high-strength concrete, longitudinal cracks could be seen in both b ng, tie rupture, and ultimately core concrete crushing. Normal-strength concrete developed surface cracks, but they did not manifest themselves as rapidly as high-strength concrete. before and after the separation of cover pieces. This behaviour is comparatively ductile as compared to concrete of the same strength.

Before the cover concrete spelling, all columns initially exhibited similar behaviour. The stress-strain relationship's ascending branches were nearly linear. In general, the ascending branches on columns made of high-strength concrete were steeper. Fewer strains were seen at the cover concrete's spelling than at the respective strengths of the long concrete columns. Fig. 11 illustrates the failure of the column under eccentric loading.

As in this work tie spacing was kept constant, and similar types of failures were observed that as the spelling of cover initially for reinforced columns, which corresponds to the first peak. After that column reaches maximum load, at which the whole cover spalls out. Then the core starts taking load which corresponds to the second peak and is less than the first peak. All the data measured during the testing of columns and individual data is also recorded for each column.

**Fig. 11** Failure of the column under eccentric loading.

The study investigated the design parameters of reinforced Ultra-High-Performance Concrete (UHPC) structural elements. UHPC was produced using locally sourced materials, with the research focusing on slender square and rectangular columns. A total of 162 UHPC columns were cast, with three specimens for each concrete grade (M60, M70, and M80). The casting process included two trial mixes to determine the optimal mix proportions for each grade.

Mechanical properties such as split tensile strength, flexural strength, and compressive strength (measured using cube and cylinder specimens) were thoroughly evaluated. The average compressive strength of UHPC increased with higher concrete grades. For example, Grade M80 achieved an experimental compressive strength of 84.14 MPa at 28 days. Similarly, the flexural and tensile strengths also improved with increasing grades. However, the experimentally obtained 28-day strengths exceeded the corresponding values specified by ACI and IS codes across all concrete grades.

A loading frame of 1000 kN capacity was employed to test slender columns under different loading conditions, ensuring precise evaluation of their behaviour. Concrete mixtures, ranging from 60 MPa to 80 MPa in strength, were prepared using a 125 kg ribbon-type mixer. The mixes were poured into plywood moulds, with exact material quantities measured per column. Initially, 75% of the total water was added to the mixer. Silica fume was mixed with dry aggregates before incorporation. The remaining 25% water was introduced later, and the mixing process continued for at least 10 minutes to ensure uniform consistency.

Workability was evaluated using the slump cone test, yielding results between 100 mm and 150 mm. Displacement measurements were recorded using Linear Variable Differential Transformers (LVDTs) and dial gauges, with one LVDT

placed on opposing faces of the specimen and another at the bottom to capture post-peak behaviour. A data acquisition system was used to automatically log displacement and load data during testing.

Axial and eccentric loading was applied using a hydraulic jack integrated into a 2000 kN loading frame, with care taken to maintain vertical alignment of the columns. Observations included initial cracking, peak load, and post-peak behaviour. These results were used to plot load-deflection curves and moment-curvature interaction diagrams, which were compared with theoretical models and past research to evaluate structural performance.

Columns were reinforced with 2.01% longitudinal steel using 8 mm diameter bars, and exhibited ductile behaviour, even under eccentric loads at 80 MPa. High-strength UHPC columns demonstrated failure modes such as longitudinal cracking, tie rupture, and core crushing, while normal-strength specimens showed slower surface crack development. Initially, the stress-strain response was linear across all grades, with a steeper curve for UHPC. After cover spalling occurred at peak load, the column's core concrete sustained additional load, often producing a secondary, lower peak. Consistent tie spacing resulted in uniform failure patterns among specimens.

All test data were logged individually, providing a detailed understanding of UHPC column performance under various loading conditions.

**6.1 Observed Behaviour of Columns:**

In the present study, twenty-seven rectangular columns were tested in axial compression. It is studied to know the effect of cover spalling concerning columns of closely spaced transverse steel. The columns S60IA1, S60IA2, S70IIA1, S80IIA3, S80IIIA2, S70IIIA3, R60IA1, R70IA3, R80IIA2, R70IIA3, R80IIIA2 and R70IIIA3 were failed in an explosive manner. They did, however, show larger compressive strains than tied columns that were closely spaced. During the SIIIA1 testing, the pi-gauges suffered complete damage and the column broke into multiple pieces.

The transverse reinforcement's stress has not yet reached its yield strength at this load. Columns will be assumed to be loaded above Pmax, which is the load corresponding to the load at which cover spalling initiates. The strength then abruptly decreases to zero in columns that are less constrained. At this point, the second peak was caused by the strengthening of the core concrete. The extent of confinement can determine whether the second peak is even higher than Pmax. The columns with 100 mm spacing were fractured suddenly after the peak load. The longitudinal bars buckled severely giving rise to explosive failure without post peak curve as shown in Fig. 5.10. At the same time columns with the same number of ties but with 2.01%, 3.14%, and 4.52% for square, similarly 1.34%, 2.09% and 3.01% for rectangular columns longitudinal steel, that is, 4# of 8mm, 4# of 10mm and 4# of 12mm, configuration have behaved comparatively in an elastic manner.

International Scientific Journal of Engineering and Management (ISJEM) ISSN: 2583-6129
Volume: 04 Issue: 08 | Aug – 2025 DOI: 10.55041/ISJEM04981
An International Scholarly || Multidisciplinary || Open Access || Indexing in all major Database & Metadata

a. (2.01 %) longitudinal reinforcement

.14 %) longitudinal reinforcement

**Fig. 12 (a-b)** Sudden buckling of longitudinal reinforcement and crushing of core of poorly confined columns

a. Development of surface cracks

b. Initiation of cover spalling

c. Separation of cover

d. Buckling of longitudinal bars

e. Opening up of ties

 

f. Rupture of ties

**Fig. 13 (a-f)** Sequence of failure of well-confined concentrically loaded columns

A significant secondary peak was observed in most of the well-confined columns. The testing concluded when the ties were broken and certain longitudinal steels experienced buckling. The sequence of failure for the well-confined and poorly-confined columns is presented in Figure 5.10. Additionally, the concentric compression tests of the columns with different tie spacing and concrete strength are displayed in Figs. 12 to 13.

**Fig.14** Rectangular Columns with longitudinal steel 3.01%, 2.09% and 1.34% for 80MPa ultra high-performance concrete

**6.2. Behaviour of Rectangular UHPC Column subjected to Uni-axial and Bi-axial loading:**

The 100 mm x 150 mm x 1300 mm rectangular Ultra High-performance concrete column has better ductility, durability, and high compressive and flexural strength, among other structural attributes. Its capacity to withstand bending moments, shear stresses, and environmental variables renders it appropriate for a range of structural applications. To fully utilize the capabilities of UHPC technology and ensure the safety, durability, and efficiency of a structure, it is crucial to employ appropriate design, construction methods, and strict adherence to structural codes.

**6.2.1 Columns Under Uni-axial Compression**

Twenty-seven column specimens of the strength of concrete 60 MPa to 80 MPa were tested by applying load uniaxially concerning the neutral axis at an eccentricity of 20% (36.36 mm) of the longer face of the column. The column was tested under uniaxial load using a loading frame of capacity 1000 kN. The load was applied by the load cell which is attached to the data acquisition system. To measure deflections two LVDTs were attached to both sides of the 150 mm face of the column. Experiential evidence demonstrates that the midspan deflection increases with an increase in applied load. When

applying the load, extra care was taken to make sure that the top and bottom ends of the column were constrained by using a bracket provided at each end. The failure pattern seen during experimentation to satisfy loading was the establishment of surface cracks, the start of cover spalling, cover breakup, buckling of longitudinal bars, opening up of ties, then finally breaking of ties. The maximum deflection for 60-80 MPa strength of concrete is 1.19 mm, while the minimum recorded 0.99 mm at the ultimate load of 573.61kN. Table 2 displays the maximum load and deflection recorded.

**Table 2** Test outcomes of Uni-axially loaded specimens.

| Grade | Reinforcement Percentage | Column Designation | Experimental Force in (kN) | Expt. Deviation (mm) | FEA Deviation (mm) | Eccentricity in (mm) | Moment (kN.m) | % Difference |
|---|---|---|---|---|---|---|---|---|
| M-60 | 1.34% | R60IU1 | 408.46 | 1.03 | 1.03 | 30 | 12.67 | 7.2 |
| | | R60IU2 | 397.64 | 0.99 | 0.99 | 30 | 12.32 | 9.9 |
| | | R60IU3 | 402.12 | 1.01 | 1.01 | 30 | 12.47 | 9.1 |
| | 2.09% | R60IIU1 | 429.12 | 1.04 | 1.04 | 30 | 13.32 | 7.3 |
| | | R60IIU2 | 431.41 | 1.04 | 1.04 | 30 | 13.39 | 3.1 |
| | | R60IIU3 | 417.67 | 1.01 | 1.01 | 30 | 12.95 | 9.1 |
| | 3.01% | R60IIIU1 | 474.12 | 1.11 | 1.11 | 30 | 14.75 | 4.4 |
| | | R60IIIU2 | 476.3 | 1.10 | 1.10 | 30 | 14.81 | 1.1 |
| | | R60IIIU3 | 468.51 | 1.09 | 1.09 | 30 | 14.57 | 8.7 |
| M-70 | 1.34% | R70IU1 | 464 | 1.08 | 1.08 | 30 | 14.42 | 3.2 |
| | | R70IU2 | 457.12 | 1.06 | 1.06 | 30 | 14.20 | 5.3 |
| | | R70IU3 | 450.90 | 1.05 | 1.05 | 30 | 14.00 | 7.4 |
| | 2.09% | R70IIU1 | 490.41 | 1.11 | 1.11 | 30 | 15.26 | 5.6 |
| | | R70IIU2 | 495.72 | 1.12 | 1.12 | 30 | 15.43 | 3.4 |
| | | R70IIU3 | 486.42 | 1.09 | 1.09 | 30 | 15.12 | 8.7 |
| | 3.01% | R70IIIU1 | 506.03 | 1.14 | 1.14 | 30 | 15.76 | 10.3 |
| | | R70IIIU2 | 511.42 | 1.12 | 1.12 | 30 | 15.92 | 5.6 |
| | | R70IIIU3 | 519.24 | 1.13 | 1.13 | 30 | 16.16 | 3.4 |
| M-80 | 1.34% | R80IU1 | 527.46 | 1.16 | 1.16 | 30 | 16.44 | 5.8 |
| | | R80IU2 | 513.90 | 1.12 | 1.12 | 30 | 15.99 | 1.1 |
| | | R80IU3 | 520.30 | 1.14 | 1.14 | 30 | 16.20 | 4.6 |
| | 2.09% | R80IIU1 | 552.90 | 1.18 | 1.18 | 30 | 17.24 | 7.1 |
| | | R80IIU2 | 549.16 | 1.16 | 1.16 | 30 | 17.11 | 9.3 |
| | | R80IIU3 | 544.26 | 1.15 | 1.15 | 30 | 16.95 | 11.5 |
| | 3.01% | R80IIIU1 | 573.61 | 1.18 | 1.18 | 30 | 17.89 | 9.4 |
| | | R80IIIU2 | 579.51 | 1.19 | 1.19 | 30 | 18.07 | 5.9 |
| | | R80IIIU3 | 568.61 | 1.17 | 1.17 | 30 | 17.72 | 2.3 |

For reinforced concrete columns of grades M-60, M-70, and M-80 with reinforcement percentages of 1.34%, 2.09%, and 3.01%, the table shows the experimental force, the greatest deviation, eccentricity, moment, and percentage difference between the experimental and FEM results. The columns were subjected to a 30 mm eccentric loading. Results indicate that as concrete grade and reinforcing % rise, so does the moment capacity of reinforced concrete columns subject to eccentric loads. The M-60 column with 1.34% reinforcement has a moment capacity of 408.46 kN.m, but the M-80 column with 3.01% reinforcement has a moment capacity of 573.61 kN.m This represents a growth of more than 40%. The Finite Element Method results exhibit a high level of accordance with the experimental results, with a maximum difference of 11.5%. These results suggest that the Finite Element Method model is capable of properly calculating the moment capacity of reinforced concrete columns when subjected to eccentric loads. With this knowledge, reinforced concrete columns may be designed for a range of loading scenarios.

### 6.2.2. Columns Under Bi-axial Compression.

A total of twenty-seven column specimens, with concrete strength ranging from 60 MPa to 80 Mega Pascal, were subjected to biaxial loading. The load was applied eccentrically about the neutral axis, with an eccentricity of 20% in both directions, resulting in a diagonal deformation of 36.36 mm. The column experienced bi-axial load testing utilizing a loading frame with a capacity of 1000kN. The load was applied using a load cell that was connected to the data acquisition system. Two Linear Variable Differential Transformers were attached to opposite sides of the 150 mm face of the column to measure deflections. Research demonstrates that as the applied stress increases, it also increases the midspan deflection.

Using the brackets at each end, extra care was taken to ensure that the column's top and bottom ends remained restricted while applying the load. The greatest deflection observed for concrete with a strength of 60-80 MPa is 1.58 mm, while the smallest recorded deflection is 1.14 mm at the ultimate load of 541.52 kN. Table 3 presents the highest load and deflection measurements that were recorded.

The purpose of this experiment was to investigate how different levels of reinforcement % impact the maximum deflection of concrete columns when subjected to both experimental and finite element method (FEM) loading.

**Table 3. Test outcomes of bi-axially loaded specimens.**

| Grade | Reinforcement Percentage | Column Designation | Experimental Force in (kN) | Expt. Deviation (mm) | FEA Deviation (mm) | Eccentricity in (mm) | Moment (kN.m) | % Difference |
|---|---|---|---|---|---|---|---|---|
| M-60 | 1.34% | R60IB1 | 383.62 | 1.17 | 1.17 | 36.06 | 14.28 | 8.2 |
| | | R60IB2 | 377.12 | 1.14 | 1.14 | 36.06 | 14.03 | 10.3 |
| | | R60IB3 | 366.42 | 1.11 | 1.11 | 36.06 | 13.62 | 10.0 |
| | 2.09% | R60IIB1 | 397.04 | 1.15 | 1.15 | 36.06 | 14.77 | 3.5 |
| | | R60IIB2 | 389.25 | 1.13 | 1.13 | 36.06 | 14.48 | 9.0 |
| | | R60IIB3 | 393.72 | 1.14 | 1.14 | 36.06 | 14.65 | 5.7 |
| | 3.01% | R60IIIB1 | 445.84 | 1.46 | 1.46 | 36.06 | 16.73 | 10.2 |
| | | R60IIIB2 | 454.32 | 1.22 | 1.22 | 36.06 | 16.94 | 2.4 |
| | | R60IIIB3 | 457.72 | 1.27 | 1.27 | 36.06 | 17.09 | 1.3 |
| M- | 1.34% | R70IB1 | 437.46 | 1.24 | 1.24 | 36.06 | 16.32 | 6.2 |

| | | | | | | | | |
|---|---|---|---|---|---|---|---|---|
| 70 | | R70IB2 | 442.11 | 1.24 | 1.24 | 36.06 | 16.49 | 5.0 |
| | | R70IB3 | 429.72 | 1.21 | 1.21 | 36.06 | 16.02 | 8.5 |
| | 2.09% | R70IIB1 | 474.72 | 1.29 | 1.29 | 36.06 | 17.73 | 9.0 |
| | | R70IIB2 | 478.00 | 1.29 | 1.29 | 36.06 | 17.85 | 7.7 |
| | | R70IIB3 | 467.27 | 1.26 | 1.26 | 36.06 | 17.44 | 10.1 |
| | 3.01% | R70IIIB1 | 486.02 | 1.27 | 1.27 | 36.06 | 18.14 | 6.3 |
| | | R70IIIB2 | 477.62 | 1.24 | 1.24 | 36.06 | 17.82 | 7.4 |
| | | R70IIIB3 | 481.07 | 1.25 | 1.25 | 36.06 | 17.95 | 10.0 |

| | | | | | | | | |
|---|---|---|---|---|---|---|---|---|
| M-80 | 1.34% | R80IB1 | 494.33 | 1.31 | 1.31 | 36.06 | 18.47 | 10.5 |
| | | R80IB2 | 499.62 | 1.32 | 1.32 | 36.06 | 18.68 | 6.6 |
| | | R80IB3 | 501.64 | 1.33 | 1.33 | 36.06 | 18.76 | 2.7 |
| | 2.09% | R80IIB1 | 516.38 | 1.33 | 1.33 | 36.06 | 19.31 | 6.7 |
| | | R80IIB2 | 523.46 | 1.34 | 1.34 | 36.06 | 19.58 | 2.7 |
| | | R80IIB3 | 512.38 | 1.31 | 1.31 | 36.06 | 19.15 | 10.5 |
| | 3.01% | R80IIIB1 | 541.52 | 1.58 | 1.58 | 36.06 | 20.38 | 7.9 |
| | | R80IIIB2 | 536.72 | 1.32 | 1.32 | 36.06 | 20.06 | 10.6 |
| | | R80IIIB3 | 547.46 | 1.36 | 1.36 | 36.06 | 20.49 | 2.7 |

The columns underwent testing at three distinct moment levels: M-60, M-70, and M-80. The reinforcement percentage was adjusted within the range of 1.34% to 3.01%. The results indicate that the highest deviation increases as the reinforcement % and moment level increase. There are minor differences between the experimental and FEM results at the higher reinforcement percentages and moment levels, but overall, the FEM's accuracy is excellent.

## 7.0 RESULTS OF RECTANGULAR COLUMN SUBJECTED TO DIFFERENT LOADING:

### 7.1. Behaviour of long column under axial loading.

Three columns for each grade of UHPC were tested under axial loading. For **1.34%** steel the M60 long column average load is 427.15 kN and the corresponding deflection is 0.79 mm. For **2.09%** steel average load is 463.61kN and the average deflection is 0.82mm. For **3.01%** steel average load 507.87kN and average deflection 0.94mm. The load on other columns with higher-grade concrete was higher than these values. The percentage of **1.34%** steel increase in strength was observed to be 14.05% and 28.04% for 70 MPa and 80 MPa concrete respectively in comparison with 60 MPa (0.79mm) concrete. The percentage decrease in average deflection for **2.09%** as compared with 60 MPa concrete (0.82 mm) is 12.51% and 25.42% respectively. The percentage decrease in average deflection for **3.01%** as compared with 60 MPa concrete (0.94 mm) is 6.64% and 18.82% respectively. The percentage increase in Peak load and percentage decrease in average deflection as the strength of concrete increases is quite obvious as both the variables depend on the strength of the concrete. This indicates that the increase in strength of concrete increases the load-carrying capacity ACI 318-19 and at the same time its lateral deflection is also controlled. In the present research, we may conclude that the advantage of using HPC may lead to structural lead to structural stability especially for columns under eccentric loading. The ratio of maximum load and theoretical loads were also calculated as shown in Table 6.2 and the ratio was found to be nearly 0.71 except for one column of strength of 80 MPa.

The results of columns in concentric compression reveal that the use of a reduction factor of 0.85 overestimates the column

capacity by ACI 318-19 for the strength of concrete above 70 MPa. This is due to the early spalling of cover concrete. The different parameters such as the amount and yield strength of longitudinal reinforcement and the amount and spacing of transverse reinforcement are very important for the behaviour of UHPC columns.

### 7.2. Behaviour of long column under uniaxial loading.

Three columns for each grade of UHPC were tested under uniaxial loading with an eccentricity of 20 mm. For **1.34%** steel the M60 long column average load is 402.74 kN and the corresponding deflection is 0.92 mm. For **2.09%** steel average load is 426.07kN and the average deflection is 1.01mm. For **3.01%** steel average load is 472.98kN and the average deflection is 1.05mm. The load on other columns with higher-grade concrete was higher than these values. The percentage of **1.34%** steel increase in strength was observed to be 13.56% and 29.25% for 70 MPa and 80 MPa concrete respectively in comparison with 60 MPa (0.92mm) concrete. The percentage decrease in average deflection of **2.09%** as compared with 60 MPa concrete (1.01 mm) is 15.20% and 28.79% respectively. The percentage decrease in average deflection of **3.01%** as compared with 60 MPa concrete (1.05 mm) is 8.29% and 21.34% respectively. The percentage increase in Peak load and percentage decrease in average deflection as the strength of concrete increases is quite obvious as both the variables depend on the strength of the concrete. This indicates that the increase in strength of concrete increases the load-carrying capacity ACI 318-19 and at the same time its lateral deflection is also controlled. In the present research, we may conclude that the advantage of using HPC may lead to structural lead to structural stability especially for columns under eccentric loading. The ratio of maximum load and theoretical loads were also calculated as shown in Table 6.2 and the ratio was found to be nearly 0.75 except for one column of strength of 80 MPa.

The results of columns in concentric compression reveal that the use of a reduction factor of 0.85 overestimates the column capacity by ACI 318-19 for the strength of concrete above 70 MPa. This is due to the early spalling of cover concrete. The different parameters such as the amount and yield strength of longitudinal reinforcement and the amount and spacing of transverse reinforcement are very important for the behaviour of UHPC columns.

### 7.3 Results of Rectangular Column Subjected to Different Loading:

#### 7.3.1. Behaviour of long column under axial loading.

Three columns for each grade of UHPC were tested under axial loading. For **1.34%** steel the M60 long column average load is 427.15 kN and the corresponding deflection is 0.79 mm. For **2.09%** steel average load is 463.61kN and the average deflection is 0.82mm. For **3.01%** steel average load 507.87kN and average deflection 0.94mm. The load on other columns with higher-grade concrete was higher than these values. The percentage of **1.34%** steel increase in strength was observed to be 14.05% and 28.04% for 70 MPa and 80 MPa concrete respectively in comparison with 60 MPa (0.79mm) concrete. The percentage decrease in average deflection for **2.09%** as compared with 60 MPa concrete (0.82 mm) is 12.51% and 25.42% respectively. The percentage decrease in average deflection for **3.01%** as compared with 60 MPa concrete (0.94 mm) is 6.64% and 18.82% respectively. The percentage increase in Peak load and percentage decrease in average deflection as the strength of concrete increases is quite obvious as both the variables depend on the strength of the concrete. This indicates that the increase in strength of concrete increases the load-carrying capacity ACI 318-19 and at the same time its lateral deflection is also controlled. In the present research, we may conclude that the advantage of using HPC may lead to structural lead to structural stability especially for columns under eccentric loading. The ratio of

maximum load and theoretical loads were also calculated as shown in Table 6.2 and the ratio was found to be nearly 0.71 except for one column of strength of 80 MPa.

The results of columns in concentric compression reveal that the use of a reduction factor of 0.85 overestimates the column capacity by ACI 318-19 for the strength of concrete above 70 MPa. This is due to the early spalling of cover concrete. The different parameters such as the amount and yield strength of longitudinal reinforcement and the amount and spacing of transverse reinforcement are very important for the behaviour of UHPC columns.

**7.3.2. Behaviour of long column under uniaxial loading.**

Three columns for each grade of UHPC were tested under uniaxial loading with an eccentricity of 20 mm. For **1.34%** steel the M60 long column average load is 402.74 kN and the corresponding deflection is 0.92 mm. For **2.09%** steel average load is 426.07kN and the average deflection is 1.01mm. For **3.01%** steel average load is 472.98kN and the average deflection is 1.05mm. The load on other columns with higher-grade concrete was higher than these values. The percentage of **1.34%** steel increase in strength was observed to be 13.56% and 29.25% for 70 MPa and 80 MPa concrete respectively in comparison with 60 MPa (0.92mm) concrete. The percentage decrease in average deflection of **2.09%** as compared with 60 MPa concrete (1.01 mm) is 15.20% and 28.79% respectively. The percentage decrease in average deflection of **3.01%** as compared with 60 MPa concrete (1.05 mm) is 8.29% and 21.34% respectively. The percentage increase in Peak load and percentage decrease in average deflection as the strength of concrete increases is quite obvious as both the variables depend on the strength of the concrete. This indicates that the increase in strength of concrete increases the load-carrying capacity ACI 318-19 and at the same time its lateral deflection is also controlled. In the present research, we may conclude that the advantage of using HPC may lead to structural lead to structural stability especially for columns under eccentric loading. The ratio of maximum load and theoretical loads were also calculated as shown in Table 6.2 and the ratio was found to be nearly 0.75 except for one column of strength of 80 MPa.

The results of columns in concentric compression reveal that the use of a reduction factor of 0.85 overestimates the column capacity by ACI 318-19 for the strength of concrete above 70 MPa. This is due to the early spalling of cover concrete. The different parameters such as the amount and yield strength of longitudinal reinforcement and the amount and spacing of transverse reinforcement are very important for the behaviour of UHPC columns.

**7.3.3. Behaviour of long column under biaxial loading.**

Three columns for each grade of UHPC were tested under biaxial loading with an eccentricity of 28.28 mm. For **1.34%** steel the M60 long column average load is 375.72 kN and the corresponding deflection is 1.11 mm. For **2.09%** steel average load is 393.34kN and the average deflection is 1.08mm. For **3.01%** steel average load is 452.63kN and the average deflection is 1.34mm. The load on other columns with higher-grade concrete was higher than these values. The percentage of **1.34%** steel increase in strength was observed to be 16.15% and 32.68% for 70 MPa and 80 MPa concrete respectively in comparison with 60 MPa (1.11mm) concrete. The percentage decrease in average deflection for **2.09%** as compared with 60 MPa concrete (1.08 mm) is 20.33% and 31.54% respectively. The percentage decrease in average deflection of **3.01%** as compared with 60 MPa concrete (1.34 mm) is 6.39% and 19.72% respectively. The percentage increase in Peak load and percentage decrease in average deflection as the strength of concrete increases is quite obvious as both the variables depend on the strength of the concrete. This indicates that the increase in strength of concrete increases the load-carrying capacity ACI 318-19 and at the same time its lateral deflection is also controlled. In the present research, we may conclude that the advantage of using UHPC may lead to structural stability, especially for columns under eccentric

loading. The trend of increase in strength and decrease in deflection in uniaxial compression is also observed in the bi-axially loaded UHPC column. However, the 80 MPa strength bi-axially loaded column showed a steep increase in load carrying capacity ACI 318-19 to the extent of 71% increase as compared to 60 MPa concrete.

At the same time, the comparison of the uniaxially loaded UHPC column and the bi-axially loaded column is also discussed. The percentage decrease in strength of bi-axially loaded columns as compared to uniaxially loaded columns was found to be in the range of 10% to 12% for all the columns. The percentage increase in deflection is 2.5%, 7.9%, and 11.5% for 60 MPa, 70 MPa, and 80 MPa concrete as compared to their uniaxially loaded columns.

## 8.CONCLUSIONS:

The following observations were derived based on a comprehensive and methodical investigation on Ultra-High-Performance Concrete (UHPC) within the strength range of 60 MPa to 80 MPa:

1. The mechanical properties, such as cube strength, cylindrical strength, split tensile strength, and modulus of rupture, consistently increase with the rise in compressive strength of UHPC.
2. The split tensile strength, flexural strength, and modulus of elasticity show a direct correlation with compressive strength and align well with certain empirical equations proposed in various international codes.
3. Under uniaxial and biaxial loading, the failure mode typically involves the formation of surface cracks, initiation and propagation of cover spalling, detachment of cover concrete, buckling of longitudinal reinforcement, opening of ties, and eventually rupture of transverse reinforcement.
4. An evident trend was observed where an increase in peak load capacity and a reduction in average lateral deflection occur with the increase in concrete strength. This confirms that higher-strength UHPC enhances load-bearing efficiency while reducing deformations.
5. The progressive increase in load capacity and corresponding decrease in deflection were consistently noted in both uniaxial and biaxial compression tests on UHPC columns.
6. The adoption of UHPC is particularly advantageous in improving structural stability, especially for eccentrically loaded columns, including corner columns under uniaxial and biaxial conditions.
7. Upon comparing the results from IS 456:2000, ACI 318-19, and the present study, it was found that:
    - IS 456:2000 tends to be conservative, offering lower load-carrying capacity but requiring heavier sections.
    - ACI 318-19 permits higher load capacities with lighter sections.
    - The proposed results from the current research offer a balanced and economical approach, suggesting optimum section sizes with reliable performance.
8. The moment interaction curves developed for UHPC with strengths ranging from 60 MPa to 80 MPa serve as a practical design tool for estimating column capacities under uniaxial and biaxial loading, without the over-conservatism of IS 456:2000 or overestimation tendencies of ACI 318-19.
9. From both experimental testing and finite element analysis (FEA) using ANSYS, it was confirmed that increased UHPC strength leads to greater load capacity and reduced deflection for both uniaxially and biaxially loaded columns. Additionally, columns under biaxial compression exhibit more sensitivity than those under uniaxial or axial compression. The FEA outcomes closely matched the interaction curves, thus validating the experimental findings of this research.

## 9. REFERENCES:

1. Abbas, S., Nehdi, M. L., & Saleem, M. A. (2016). Ultra-high performance concrete: Mechanical performance, durability, sustainability and implementation challenges. *International Journal of Concrete Structures and Materials, 10*(3), 271–295. https://doi.org/10.1007/s40069-016-0157-4
2. Aïtcin, P. C., & Flatt, R. J. (2016). *Science and technology of concrete admixtures*. Woodhead Publishing. https://doi.org/10.1016/B978-0-08-100693-1.00023-8
3. Ahmed, S. F. U., Maalej, M., & Paramasivam, P. (2007). Flexural responses of hybrid steel–polyethylene fiber reinforced cement composites containing high volume fly ash. *Construction and Building Materials, 21*(5), 1088–1097. https://doi.org/10.1016/j.conbuildmat.2006.01.003
4. ASTM C1856/C1856M-17. (2017). *Standard practice for fabricating and testing specimens of ultra-high performance concrete*. ASTM International. https://doi.org/10.1520/C1856_C1856M-17
5. Bogas, J. A., Real, S., & Ferrer, B. (2021). Steel fibre reinforced UHPC: Mechanical properties and impact of fibre geometry. *Construction and Building Materials, 269*, 121308. https://doi.org/10.1016/j.conbuildmat.2020.121308
6. Charron, J. P., Denarié, E., & Brühwiler, E. (2008). Permeability of ultra high performance fiber reinforced concretes (UHPFRC) under high stresses. *Materials and Structures, 41*(2), 269–279. https://doi.org/10.1617/s11527-007-9236-0
7. Graybeal, B. A. (2006). *Material property characterization of ultra-high performance concrete*. FHWA-HRT-06-103, Federal Highway Administration.
8. Graybeal, B. A. (2008). Flexural behavior of an ultrahigh-performance concrete I-girder. *Journal of Bridge Engineering, 13*(6), 602–610. https://doi.org/10.1061/(ASCE)1084-0702(2008)13:6(602)
9. Graybeal, B., & Tanesi, J. (2007). Durability of an ultra high performance concrete. *Journal of Materials in Civil Engineering, 19*(9), 848–854. https://doi.org/10.1061/(ASCE)0899-1561(2007)19:9(848)
10. Guan, X., Shi, C., & Zhang, Z. (2021). Compressive behaviour of ultra-high performance concrete under axial loading. *Construction and Building Materials, 272*, 121636. https://doi.org/10.1016/j.conbuildmat.2020.121636
11. Habel, K., Denarié, E., & Brühwiler, E. (2006). Experimental investigation of composite ultra-high-performance fiber-reinforced concrete and conventional concrete members. *ACI Structural Journal, 103*(1), 93–101.
12. Kang, S. T., & Kim, J. K. (2011). The relation between fiber orientation and tensile behavior in an ultra high performance fiber reinforced cementitious composites (UHPFRCC). *Cement and Concrete Research, 41*(10), 1001–1014. https://doi.org/10.1016/j.cemconres.2011.05.012
13. Kim, D. J., Park, S. H., Ryu, G. S., & Koh, K. T. (2011). Comparative flexural behavior of hybrid ultra high performance fiber reinforced concrete with different macro fibers. *Construction and Building Materials, 25*(11), 4144–4155. https://doi.org/10.1016/j.conbuildmat.2011.04.051
14. Li, Z., Wu, C., & Shi, C. (2018). Shear behaviour of steel–UHPC composite beams. *Engineering Structures, 168*, 247–257. https://doi.org/10.1016/j.engstruct.2018.04.086
15. Markovic, I. (2006). *High-performance hybrid-fibre concrete: Development and utilization*. Delft University Press.
16. Naaman, A. E., & Wille, K. (2012). The path to ultra-high performance fiber reinforced concrete (UHP-FRC): Five decades of progress. *Proceedings of the 2nd International Symposium on Ultra-High Performance Concrete*, 3–15.
17. Richard, P., & Cheyrezy, M. (1995). Composition of reactive powder concretes. *Cement and Concrete Research, 25*(7), 1501–1511. https://doi.org/10.1016/0008-8846(95)00144-2
18. Shi, C., Wu, Z., Xiao, J., Wang, D., Huang, Z., & Fang, Z. (2015). A review on ultra high performance concrete: Part I. Raw materials and mixture design. *Construction and Building Materials, 101*, 741–751. https://doi.org/10.1016/j.conbuildmat.2015.10.088
19. Wille, K., Naaman, A. E., & Parra-Montesinos, G. J. (2011). Ultra-high performance concrete with compressive

strength exceeding 150 MPa (22 ksi): A simpler way. *ACI Materials Journal, 108*(1), 46–54.

20. Yoo, D. Y., Banthia, N., Yoon, Y. S., & Kim, J. J. (2016). Predicting flexural response of ultra-high-performance fiber-reinforced concrete beams. *Cement and Concrete Composites, 70*, 153–165. https://doi.org/10.1016/j.cemconcomp.2016.03.014

**BIOGRAPHIES (Optional not mandatory )**

| | |
|---|---|
|  | Dr. Bajirao V. Mane is currently pursuing his Post Doctoral Programme in the Department of Civil Engineering, Srinivas University, Institute of Engineering & Technology, Srinivas Nagara, Mukka, Mangaluru, Karnataka, 574146, India. He holds a Doctoral degree from the Department of Civil Engineering, School of Engineering and Technology, DYPU, Ambi, Pune, 410506, India. Currently, he working as an Assistant Professor in the Department of Civil Engineering, Annasaheb Dange College of Engineering and Technology, Ashta, Sangli, 416301, India, since the year 2020. His field of specialization is High-Performance Concrete, Design of Reinforced Concrete Structures, and Finite Element Analysis. He has published 5 articles in reputed peer-reviewed National and International Journals and 6 in Edited Books. He has attended/presented research papers in various Seminars, Conferences, and workshops at National and International levels. |
|  | Dr. Praveen B. M. is a Director of the Research and Innovation Council at Srinivas University, Institute of Engineering & Technology, Srinivas Nagara, Mukka, Mangaluru, Karnataka, 574146, India. He holds a Post Doctorate from IISc and South Korea. He has published more than 121 articles in reputed peer-reviewed National and International Journals. He has attended/presented research papers in various Seminars, Conferences, and workshops at National and International levels. He has also organized various seminars and workshops at the National and International levels. Under his supervision and guidance, more than 10 Ph.D. degrees were awarded and 5 are pursuing Ph.D. He has made significant contributions to research in the fields of Electrochemistry, Nanocomposites, Electrodeposition, and Corrosion. |
|  | Dr. Amit Prakash Patil is an Associate Professor at the Department of Civil Engineering, Rajarambapu Institute of Technology Rajaramnagar, Islampur, Tal. Walwa, Dist. Sangli, Maharashtra, India - 415414. India. He holds a Doctorate from NITK Surathkal. He has published more than 25 articles in reputed peer-reviewed National and International Journals. He has attended/presented research papers in various Seminars, Conferences, and workshops at the National and International level. He has also organized various seminars and workshops at the National and International levels. Under his supervision and guidance, 2 Ph.D. degrees were awarded and 3 are pursuing Ph.D. He has made significant contributions to research in the field of Artificial intelligence in civil engineering, water resource engineering, Construction Tech, and Management. |